# Inelastic damages by stress wave on steel surface at the incubation stage of vibration cavitation erosion

Chen Haosheng*, Liu Shihan

*State Key Laboratory of Tribology, Tsinghua University, Beijing 100084, China*

## ARTICLE INFO

## ABSTRACT

In cavitation erosion, stress waves will be generated and propagated in the solid when a collapse impingement is acted on it. The cavitation damages on the solid surface are considered to be under the effect of the stress waves. An ultrasonic vibration cavitation erosion experiment was performed on a polished steel specimen, and not only the plastic deformations but also the brittle fractures appeared on the surface at the incubation stage of cavitation erosion. Some characteristics such as the hemispherical shape of the crater, intergranular fractures and subsurface comminution make the damages distinguishable from the common plastics deformations, and they are thought to be the results of shear waves. Thus, stress waves are proved to take part in the cavitation erosion, and they bring some special damage styles depending on the conditions of the impaction and mechanical properties of the specimen.

© 2008 Elsevier B.V. All rights reserved.

## 1. Introduction

It has been proved in experiments [1,2] and from numerical results [3,4] that the impact of a micro-jet formed at the moment of cavity collapse has a major role in causing erosion on neighboring solid materials. It is believed that the potential energy of a cavity is transferred into the micro-jet through collapse. Recently, there are many attempts to predict the magnitude of the cavitation erosion based on the energy transfer model, such as the phenomenological model using destructive pressure pulses [5], a developed model using emitted pressure wave [6], the relationship between the volume of transient cavities and its rate of production to the material deformation energy [7], and so on. Most of the models are based on the viewpoint [8] that the energy is absorbed by the plastic deformation of the specimen surface, and a deformed surface is the characteristic of the cavitation erosion at its incubation stage.

However, such models are incomplete because the plastic deformation is not the only response of metal especially under a hypervelocity impaction. For example, it is known that impulsive loading can cause a normally ductile metal to fracture in a brittle manner [9], and in Rinehart's study [10], damages by plastic deformations of the ductile metal are even absent under an hypervelocity impaction. On the other hand, stress waves will be generated in solid when collapse impingement acts on its surface, and the stress

waves are considered to have an important role in the material damage [11]. The damages caused by the stress waves on an elastic material and a rigid-perfectly plastic solid have been studied by Grant [12] and Lush [13] using liquid impact, respectively. Also, stress wave has been considered in cavitation erosion models mentioned above [5,6], although its effect is constraint to cause plastic deformations.

In this undergoing study, the characteristics of the surface damages under stress waves by collapse impingement are focused on after a vibration cavitation experiment. Such investigation on the damages may help us understand the mechanism of the cavitation erosion more completely.

## 2. Experimental

### 2.1. Schematics and apparatus

Fig. 1(a) shows the schematic of an ultrasonic vibration cavitation apparatus used in the experiment. The experiment is performed in a beaker filled with de-ionized water. The vibratory amplifying horn performs an axial vibration with frequency of 20 kHz and amplitude of 6 μm. The specimen is fixed on the support arm of a two-dimensional table at a small distance from the horn, and the interval between them can be adjusted by the translation stage.

The specimen is designed according to the Chinese standard (GB6383-86) on vibration cavitation erosion system, and its picture is shown in Fig. 1(b). The specimen is made of medium carbon steel

* Corresponding author. Fax: +86 010 62781379.
  *E-mail address:* chenhs@mail.tsinghua.edu.cn (C. Haosheng).
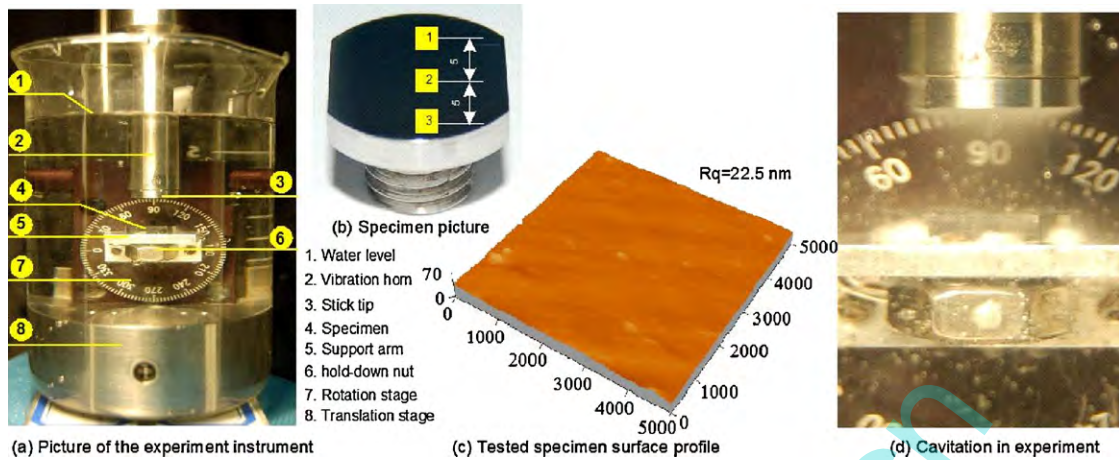
**Fig. 1.** (a) Schematics of the vibration cavitation erosion system, (b) the specimen, (c) surface profile of the specimen tested by AFM, and (d) cavitation and cavities during the experiment.

(0.45% carbon), whose yield stress $\sigma_s$ is higher than 355 MPa, the ultimate tensile stress $\sigma_b$ is higher than 650 MPa. Its chemical composition is shown in Table 1. The specimen surface is polished, and the mean squared surface roughness (Rq) is $28 \pm 5.6$ nm, which is tested by an Atomic Force Microscope (AFM) CSPM 4000. It should be noted here that the surface roughness is the mean value of the three measuring regions marked as 1–3 on the specimen surface in

**Table 1**
Chemical composition of 45# carbon steel (%)

| C | Si | Mn | P | S | Cr | Ni | Cu | Fe |
|---|---|---|---|---|---|---|---|---|
| 0.37–0.44 | 0.17–0.37 | 0.50–0.80 | 0.021 | 0.001 | 0.80–1.10 | 0.126 | 0.15 | others |
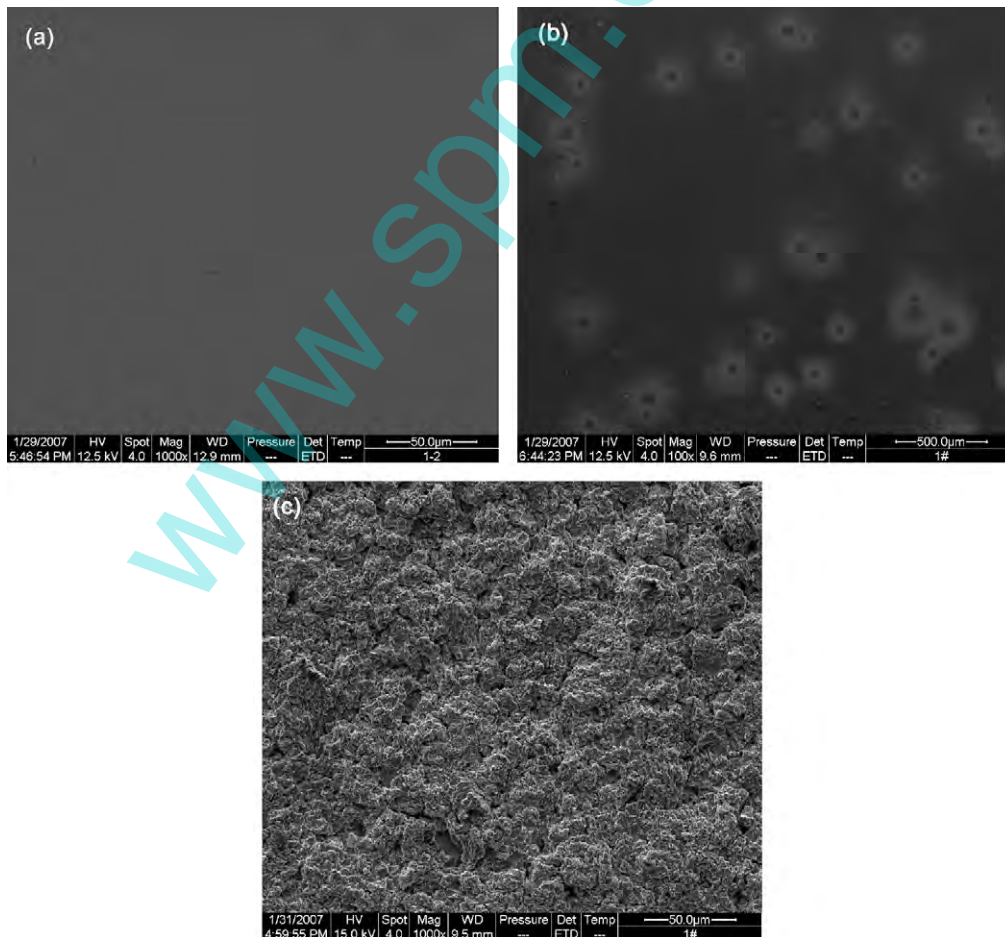


**Fig. 2.** (a) The clean specimen surface before experiment, (b) the surface after 1-minute experiment with some independent pits on it, (c) the severe damaged surface after 90-minutes experiment.
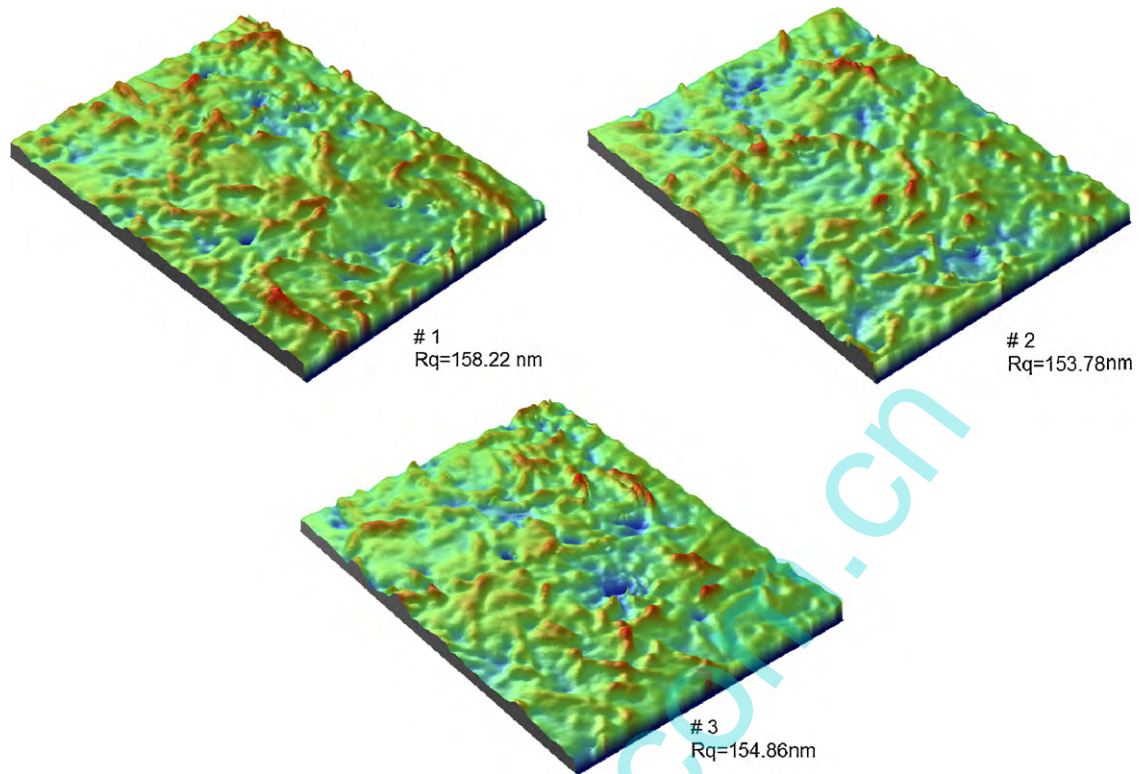
Fig. 3. Surface profiles of specimen under Wyko optical interferometer after 1-minute experiment. #1–#3 correspond to the measuring regions 1–3, respectively.

Fig. 1(b). Fig. 1(c) shows the surface profile of one of the measuring regions.

As shown in Fig. 1(d), a clear cavitation domain was found near the vibration horn's tip, and cavities were seen rush to the specimen surface. Pictures shown as Fig. 2(a–c) represent the specimen surfaces acquired by Scanning Electron Microscope (SEM, Quanta 200 FEG, FEI Co.) after the experiments with the duration of 0 s, 1 min and 90 min, respectively. To study the mechanism of cavitation erosion at the incubation stage, the duration of experiment should satisfy two conditions: (a) it should be long enough to obtain single-impact damage characteristics; (b) it should be short enough to avoid impact damage superposition. Independent pits on the surface shown in Fig. 2(b) indicate that 1 min is a proper duration. Such pits are usually called needle-like pits, which is a characteristic phenomenon appeared at the incubation stage of the cavitation erosion as described by Hammit [14], and it is considered as the result of the impingement of the collapse of cavities.

### 2.2. Plastic deformation

It was commonly recognized that the cavitation erosion would result in a heavily deformed surface at the incubation stage [8]. In this experiment, a same result was also acquired. After the experiment, undulations and craters appeared on the surface, which were measured by Wyko MHT-III optical interferometer and shown in Fig. 3. The undulations and craters belong to the plastic deformations, they increase the surface roughness, and they are considered as the main damage style at the incubation stage. The relationship between the deformation and the strength of the stress waves has already been represented by Dular's model [6].

Crater is usually a result of surface material deformation, but the shearing wave is considered to take part in the formations of some craters appeared in this experiment. Fig. 4(a) shows one of the craters observed by an Olympus LEXT OLS3100 confocal laser

scanning microscope. The surface profile of the crater at the A–A cross-section is shown in Fig. 4(b).

The crater has an almost hemispherical shape according to the surface profile curve, which is also validated by Fig. 5(a) and (c), the
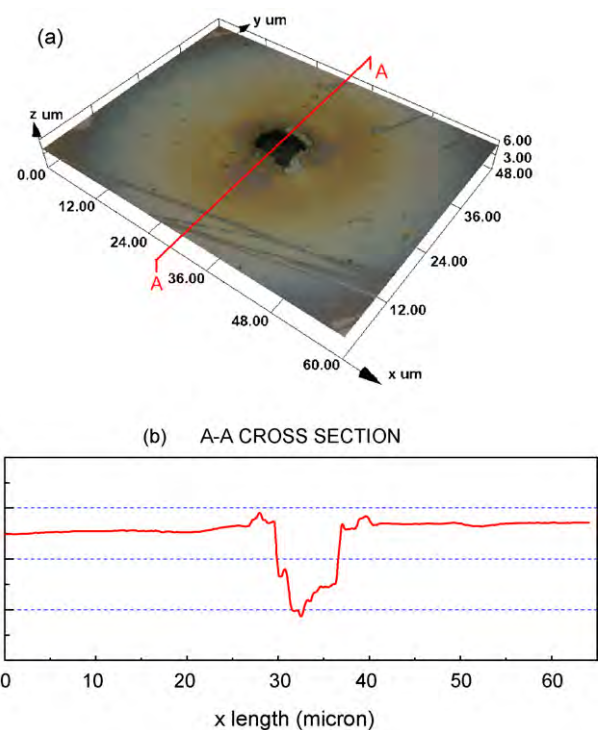


Fig. 4. (a) A crater observed by confocal laser scanning microscope, (b) surface profile of the crater at the cross-section A–A.
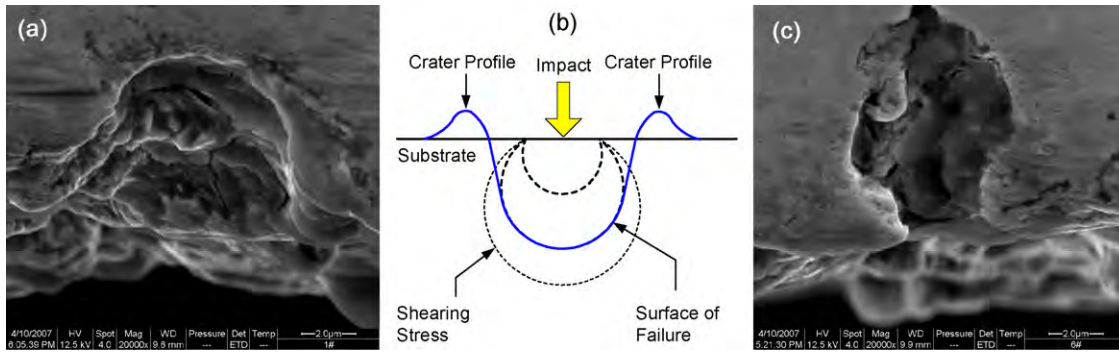
**Fig. 5.** In (a) and (c) the cross-section of craters is shown, (b) is the distribution of shear stress and crater formation.

SEM pictures of the crater's cross-sections acquired by linear cutting. The rim of the crater is obvious, which shows a plastic flow of material. According to the viewpoint [15,16], both the crater and the rim correspond to the plastic deformations under the impingement of the collapse of a cavity.

However, the volume of the rim is much less than that of the hollow, which indicates that the plastic deformation is not the only reason for the formation of the crater. Here, a hypervelocity impaction model provided by Rinehart and Pearson [10] is adopted to give a more reasonable explanation. With Rinehart's point of view, when a specimen is under an impulsive impaction, it will fail within a region in which the shearing stress exceeds a certain crit-

ical value. The distribution of shearing stress is approximately that shown in Fig. 5(b) when a semi-infinite specimen is subjected to a hypervelocity impaction.

Each of the circles in the figure corresponds to the intercept of a surface of constant shearing stress. The magnitude of the shearing stress decreases with distance from the impacting point. There will be a surface of failure when a shear stress corresponds to the critical limiting sharing stress discussed in Section 2. According to the different impaction energy, the crater would have approximately the shape of the surface of failure, which can be seen from the shapes of the craters shown in Fig. 5(a) and (c). At the same time, material would be pushed upward and outward to form the rim if the stress
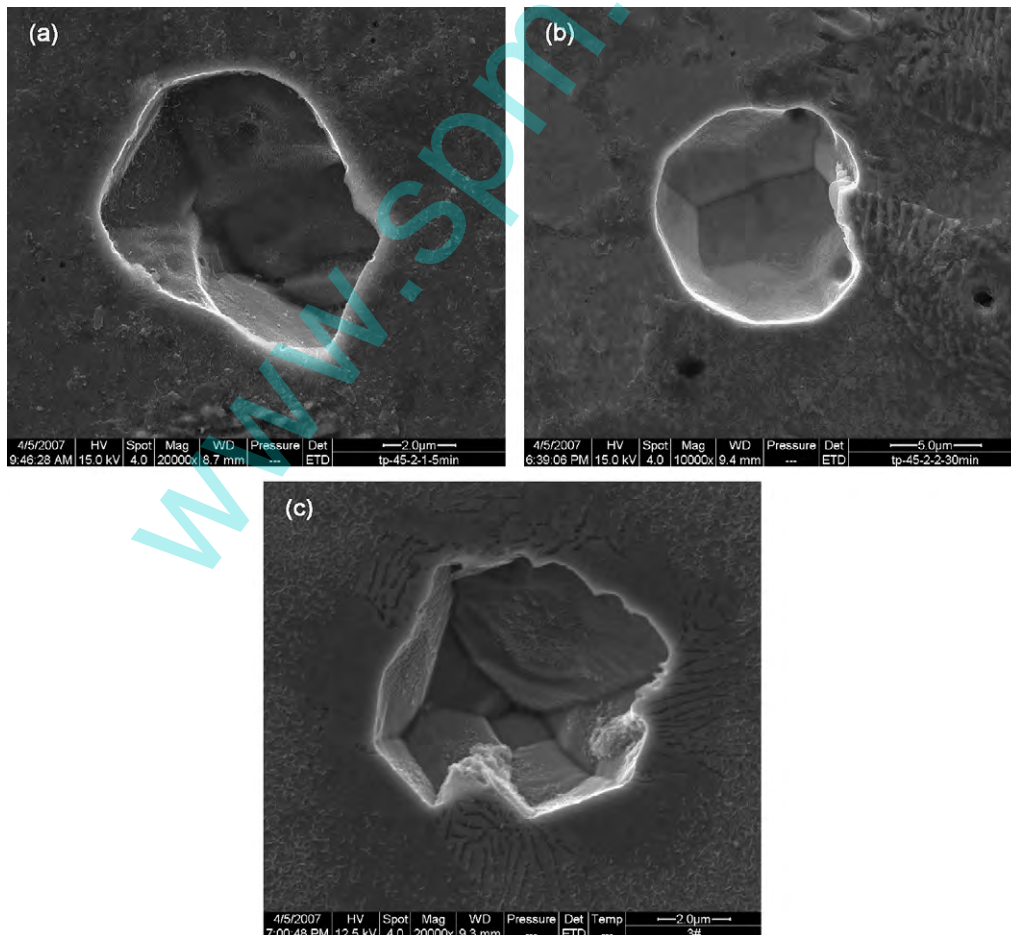


**Fig. 6.** Brittle intergranular fractures on the specimen surface observed by SEM.
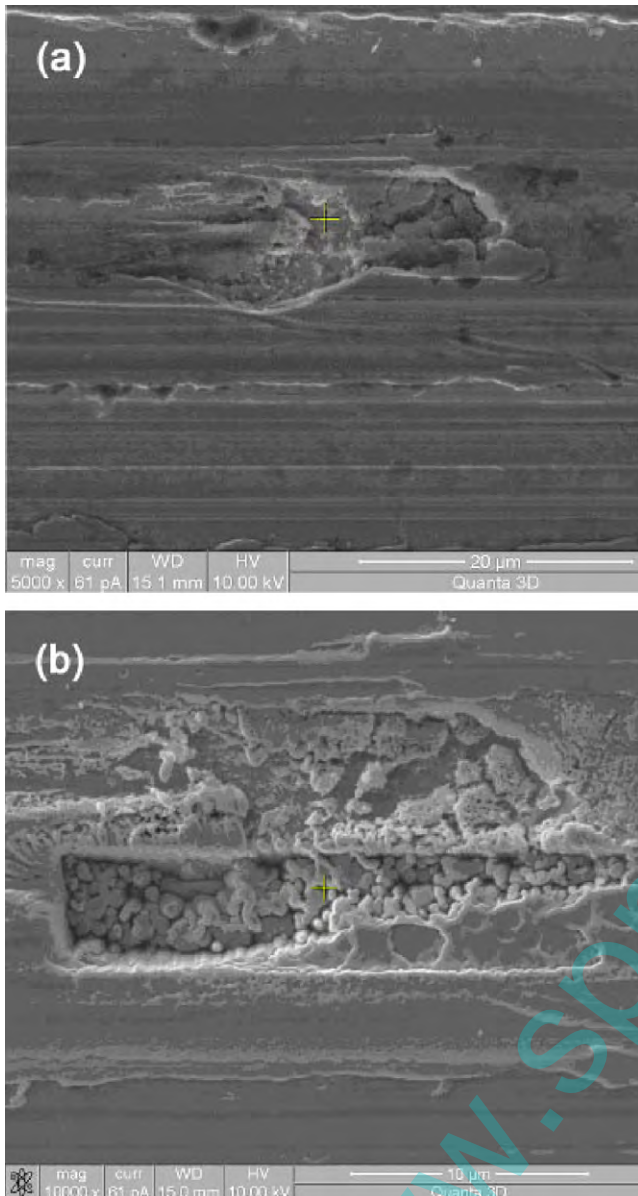
**Fig. 7.** Comminution in subsurface layer observed by FIB. (a) Surface damage, (b) subsurface damage.

overcomes the yield stress of the material near the free surface of the specimen. Otherwise, there would be little deformation of the material near the free surface, which is shown in Fig. 5(c). Thus, it is believed that the shape of some craters is the superposition of the damages in region (I) and (III). However, it should be noted that not all the craters are formed under the combined effect of different waves.

### 2.3. Fracturing

Besides the plastic deformation, the motions of particles caused by waves may loose or even destroy the structure of the metal grains. The damage often begins from the micro-cracks in the body of the metal, especially from the grain boundaries. If the stress is higher than the critical failure stress of fracture discusses above, the fracture of the structure will happen.

Usually, fractures include brittle fracture and ductile fracture. In most cases, a brittle fracture does not happen in a ductile metal. But

under special circumstances, such as impact loading, a normally ductile material fractures in a brittle manner. It has been proved that shear waves generated under hypervelocity impact can cause brittle fractures with slight plastic deformation on a target [10]. The brittle fractures were also found in this experiment and were shown in Fig. 6. The grain boundaries and grain planes were clear in the damage region, which indicates that it is an intergranular fracture. Most of the intergranular fractures are brittle fractures, and it was validated by the fact shown in Fig. 6 that the broken surfaces were bright and granular, with no apparent associated plastic deformation.

Causing damage in subsurface layer of a specimen is a special ability of stress wave. Fig. 7(a) shows a damaged region where the surface still exists. When the subsurface material was examined using focusing ion beam (FIB), it was found in Fig. 7(b) that the subsurface material structure was severely damaged. The metal structure is completely destroyed and the material changed into comminuted powder. It indicates that the subsurface damage may be more severe than that on the surface. Although the mechanism of the subsurface comminution is still obscure, the interference of stress waves and the reflected waves from boundaries is thought to have the possibility to cause such damages [11,17].

In brief, although some special damages, such as the intergranular fracture and the comminution, are not the main damage style on the specimen, the occurrence of them indeed proves that the stress waves have taken part in the surface damages at the incubation stage of cavitation erosion.

## 3. Discussions

It is commonly recognized that an impulsive loading will be generated by collapse impingement during cavitation erosion. An impulsive load is characterized by its suddenness of application and brevity of duration. As a result, stress wave is generated and propagates in the specimen. Its intensity is of sufficient magnitude to produce fracturing and permanent distortions in the specimen. The basic features of wave propagation in an elastic half-space are described in Fig. 8 according to Miller and Pursey's study [18,19]. Two basic types of waves, body waves and surface waves, are generated according to elastic half-space theory. The body waves are the compression wave and the shear wave, and the surface wave is Rayleigh wave. Body waves propagate radially outward from the source along hemispherical wave fronts, and the Rayleigh wave propagates radially outward on a cylindrical wave front. The particle motions of different waves are described in detailed in the classical work [20].

But steels are usually elastic-plastic materials [10]. The material with an elastic-plastic constitutive relation will produce elastic and plastic strains. The deviator strain $e_{ij}$ is decomposed into elastic and plastic parts as shown in Eq. (1), where the superscript e represents the elastic while p represents the plastic.

$$e_{ij} = e_{ij}^{e} + e_{ij}^{p} \tag{1}$$

It means that a plastic wave will be generated after the elastic wave when the pressure of the impingement is higher than the yield point of the steel, so the energy will be absorbed by two parts: one is the plastic deformation of the materials on the surface, and the other is the waves propagate and attenuated in the materials. It is commonly thought that the plastic deformation is the main way for the metal to absorb the impingement energy, but here the stress waves, especially the shearing stress, are also considered to take effects on the fracture at the incipient stage of cavitation erosion according to the brittle fracture found in the experiment. The crater and the fracture are both inelastic failures, whether a material will
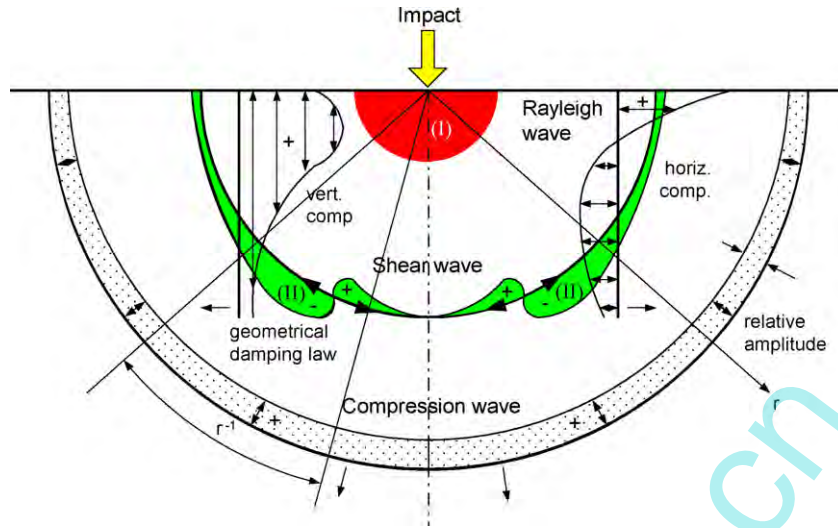
**Fig. 8.** Distribution of the stress waves in elastic half-space, and the different damage regions by the stress waves.

deform plastically or fracture in brittle type depends on both the conditions of loading and the properties of materials.

### 3.1. Plastic deformation by micro-jet

When the pressure of the impingement is higher than the yield point of the steel, a plastic wave is generated after the elastic wave. When the material has a good ductility, it performs a plastic flow and then a pit or crater is produced. Such pit is generally the result of one impingement, and the position is just the point where the impingement loading, which is marked as region (I) in Fig. 8. To cause the plastic deformation, the pressure $P_Y$ needs to satisfy the Von Mises yield condition [9].

$$P_Y = \frac{2}{3}Y, \quad \text{where } Y = Y_0 = \sqrt{3}\sigma_s \tag{2}$$

In the Eq. (2), $\sigma_s$ is the yield stress in shear, and $Y_0$ is equal to the yield stress in simple tension. For a material exhibiting work hardening property, such as the mild carbon steel, $Y$ is not constant, and a simplified expression for $Y$ is assumed, $Y = Y_0 + ke^p$ [10]. Thus, the constitutive equations can be reduced to Eq. (3).

$$P_Y = \frac{2}{3}(Y_0 + ke^p) \tag{3}$$

If the micro-jet has sufficient velocity to generate a pressure greater than $P_Y$, a plastic wave will also propagate behind the elastic wave, and the plastic deformation will occur on the specimen's surface. The radius of the region (1) $r_{pit}$ can be calculated according to Eq. (4) provided by Dular [6]. In the equation, $d$ is the depth of the pit, $v$ is the velocity and c is the sonic velocity, $k_1$ is a material related constant and usually lies between 15 and 30. The subscript 'pit' means the pit caused by the impingement, 'jet' represents the micro-jet at the moment of bubble collapse, 'def' represents the material deformation. This equation clearly shows the influence of the impingement and the material on the formation of the pit.

$$r_{pit} = k_1 \cdot d_{pit}, \quad \text{where } d_{pit} = \frac{v_{def} \cdot r_{jet}}{c} \tag{4}$$

### 3.2. Fracturing by shear waves

Just as Kristensen pointed out in his work [8], not all the energy was absorbed by the plastic deformation of the materials. Part of the energy changes into the stress waves propagating in the materials, among which the shear wave occupies 26% of the energy [19].

Although the shearing stress may not be high enough to cause the plastic deformation, it takes great effect on the erosion through causing fracture. It is known that the strength of the steel grain boundaries is much lower, and micro-cracks exist in the boundaries. When the energy of the shear wave is high enough to break the grain boundaries, the cracks grow along the grain boundary and an intergranular fracturing will happen at last. The fracturing by shear stress is marked as region (II) in Fig. 8.

According to the Griffith energy criterion for fracture [21], fracture occurs when the energy available for crack growth is sufficient to overcome the resistance of the material. For a crack with the length of $a$, there is a critical failure stress $\sigma_c$. When the stress applied is higher than the critical failure stress, the crack grows rapidly and drives the material to fracture at last. For brittle material, the expression of the critical failure stress is as Eq. (5), where $E$ is the elastic modulus, $\gamma_s$ is the surface energy of the material.

$$\sigma_c = \sqrt{\frac{2E\gamma_s}{\pi a}} \tag{5}$$

Thus, the fracture may occur at the same time of the plastic deformation when the surface cannot absorb the whole impingement energy. But not as the formation of the pit, the formation of fracture can be caused by many impacts, whose pressure can be lower than the yield point of the material. The fracturing position can be also different from profile of the shear wave, while it copes with the line where the intergranular crack grows. As a result, the fracture often causes the departure of a whole grain from the surface, which is the main phenomenon distinguished from the plastic deformation in the experiment.

## 4. Conclusions

Vibration cavitation erosion experiments were performed on polished steel surfaces. Characteristics of the damaged surface show that stress waves generated by the hypervelocity impaction play an important role in the cavitation erosion at the incubation stage. Some of the conclusions are drawn as follows:

(1) Plastic deformation is not the only damage style on the steel surface at the incubation stage of the cavitation erosion. Brittle fractures by the shear waves also happen in the stage under the hypervelocity impaction, and it is validated by the special dam-

ages such as the intergranular fracturing and the subsurface comminution on the specimen.

(2) According to the stress wave models in the elastic half-space, the plastic deformation is thought to be caused by the plastic flow of the material as the impingement pressure is higher than the yield point of the material, while the fracture is originated from the intergranular cracks at the grain boundaries by the shear waves.

## Acknowledgments

## References

[1] C.L. Kling, A high speed photographic study of cavitation bubble collapse, Ph.D. thesis, University of Michigan, 1970.

[2] N.D. Shutler, R.B. Mesler, A photographic study of the dynamics and damage capabilities of bubbles collapsing near solid boundaries, Trans. ASME, J. Basic Eng. 87 (1965) 511–517.

[3] H.C. Yeh, W.J. Yang, Dynamics of bubbles moving in liquids with pressure gradient, J. Appl. Phys. 19 (1968) 3156–3165.

[4] M.S. Plesset, R.B. Chapman, Collapse of an initially spherical vapor cavity in the neighborhood of a solid boundary, J. Fluid Mech. 47 (1971) 283.

[5] A. Karimi, W.R. Leo, Phenomenological model for cavitation erosion rate computation, Mater. Sci. Eng. 95 (1987) 1–14.

[6] M. Dular, B. Stoffel, B. Sirok, Development of a cavitation erosion model, Wear 261 (2006) 642–655.

[7] F. Pereira, F. Avellan, P. Dupont, Prediction of cavitation erosion: an energy approach, J. Fluids Eng. 120 (4) (1998) 719–727.

[8] J.K. Kristensen, I. Hansson, K.A. Mϕrch, A simple model for cavitation erosion of metals, J. Phys. D: Appl. Phys. 11 (1978) 899–912.

[9] P.C. Zhou, A.K. Hopkins, Dynamic response of materials to intense impulsive loading. 1973, printed in U.S.A. Air Force Materials Laboratory (USA), Ohio.

[10] J.S. Rinehart, J. Pearson, Behavior of Metals under Impulsive Loads, American society for metals, Cleveland, Ohio, 1954.

[11] H.H. Shi, K. Takayama, N. Nagayasu, The measurement of impact pressure and solid surface response in liquid–solid impact up to hypersonic range, Wear 186–187 (1995) 352–359.

[12] M.McD. Grant, P.A. Lush, Liquid impact on a bilinear elastic-plastic solid and its role in cavitation erosion, J. Fluid Mech. 176 (Mar) (1987) 237–252.

[13] P.A. Lush, Impact of a liquid mass on a perfectly plastic solid, J. Fluid Mech. 135 (1983) 373–387.

[14] F.G. Hammitt, Cavitation and Multiphase Flow Phenomena, McGraw-Hill Inc., USA, 1980, pp: 241.

[15] A. Karimi, F. Avellan, Comparison of erosion mechanisms in different types of cavitation, Wear 113 (1986) 305–322.

[16] A. Karimi, R.K. Schmid, Ripple formation in solid–liquid erosion, Wear 156 (1992) 33–47.

[17] M.I.A. Othman, Y. Song, Reflection of plane waves from an elastic solid half-space under hydrostatic initial stress without energy dissipation, Int. J. Solids Struct. 44 (2007) 5651–5664.

[18] G.F. Miller, H. Pursey, On the partition of energy between elastic waves in a semi-infinite solid., Proc. Royal Soc., London, A 233 (1955) 55–59.

[19] R.D. Woods, A.M. ASCE, Screening of surface waves in soils, J. Soil Mech. Found. Div. 7 (1968) 951–979.

[20] Graff, F. Karl, Wave Motion in Elastic Solids, Clarendon Press, Oxford, 1975.

[21] T.L. Anderson, Fracture Mechanics: Fundamentals and Applications, CRC Press, Boca Raton, 1995.